Chi-Phase Formation During Soldification and Cooling of CF-8M Weld Metal

A Fe, Cr, Mo intermetallic compound is found to form in the GTA weld metal of a casting alloy that is similar to Type 316 stainless steel

BY M. J. CIESLAK, A. M. RITTER, AND W. F. SAVAGE

ABSTRACT. Chi phase (an Fe, Cr, Mo intermetallic compound) was found in weld metal of alloy type CF-8M, a stainless steel casting alloy similar to Type 316 stainless steel. This phase formed during cooling of the weld metal made by autogeneous gas tungsten arc (GTA) welding using various combinations of argon/nitrogen shielding gases.

Chi phase formed in the solid state in welds that solidified in the primary austenite/eutectic ferrite solidification mode. The chi precipitates nucleated at the austenite/eutectic ferrite interfaces. A morphologically distinct form of chi phase was found as an eutectic consitutent along solidification grain boundaries in welds which solidified either as primary austenite or as primary delta-ferrite.

Introduction

Chi phase is an intermetallic compound containing primarily Fe, Cr, and Mo. It is a body-centered-cubic phase (α-Mn structure), with a lattice parameter of $a_o = 8.920$Å (Ref. 1). Chi phase is often found in austenitic and ferritic stainless steels that contain molybdenum (Refs. 2–14). This precipitate has been found previously in specimens which underwent long time, high-temperature heat treatments (Refs. 2–12).

Literature Review

Leitnaker (Ref. 2) reported the appearance of chi phase in castings of Fe-16Cr-8Ni-2Mo heat-treated for 1000 hours (h) at 732°C (1350°F) and for 5000 h at 649°C (1200°F). This alloy had a Mo content of 1.64 wt-% and a Ferrite Number of 4.5 in the as-cast condition. No chi phase was found in the as-cast condition.

Lai and Haigh (Ref. 3) found no evidence of chi phase in the as-welded duplex microstructure of Fe-18Cr-11Ni-2.5Mo. Abundant chi phase was found precipitating at the austenite/delta-ferrite interfaces after a 1 h heat treatment at 750 or 800°C (1382 or 1472°F). The composition of their weldments and morphology of the retained delta-ferrite suggest a primary delta-ferrite solidification mode.

Weiss and Stickler (Ref. 4) determined a time-temperature-precipitation (TTP) diagram for chi phase in Type 316 and 316L austenitic stainless steels. These wholly austenitic alloys were in the solution-annealed condition prior to heat treatment. The earliest occurrence of chi phase in Type 316L stainless steel was after a 1 h heat treatment at 816°C (1501°F). The earliest occurrence of chi phase in the Type 316 alloy was after heat treatment for 100 h at 816°C (1501°F). The Type 316L material had a higher Mo content than did the Type 316 heat (2.66 vs. 2.05 wt-%) that may have accounted for the difference in precipitation kinetics.

Wiegand and Doruk (Ref. 5) stated that carbon does not retard the precipitation of chi phase in austenitic stainless steels. Thier *et al.* (Ref. 6) reported that chi phase can dissolve up to 0.24 wt-% carbon, but only 0.007 wt-% nitrogen and that nitrogen additions delay chi phase precipitation. Sprueill *et al.* (Ref. 7) found chi phase in Type 316 stainless steel which had been cold rolled 20% after a 1 h anneal at 1050°C (1922°F), and subsequently heat treated for 1359 h at 710°C (1310°F).

Grot and Sprueill (Ref. 8) found chi phase in Type 316 stainless steel which was titanium-stabilized. The alloy was fully solution-annealed, swaged to a reduction in area of 10%, and heat treated at 770°C (1418°F) for 20 h. Hull reported (Ref. 9) that large amounts of chi phase were found in levitation melted,* chill-cast specimens of a variety of molybdenum-containing austenitic stainless steels after heat treating at 816°C (1501°F) for 1000 h. No chi phase was found in the as-cast condition.

Chi phase also forms in the solid state in ferritic stainless steels. Streicher (Ref. 10) reported the occurrence of chi phase in fully annealed Fe-29Cr-4.3Mo and Fe-28.5Cr-4.2Mo-2.0Ni in less than 1 h at 815°C (1499°F). Kiesheyer and Brandis (Ref. 11) reported that chi phase occurs in fully annealed 20Cr-5Mo, 24Cr-5Mo, and 28Cr-5Mo ferritic stainless steels in times of less than 6 minutes (min) in the temperature range of 750–925°C (1382–

Paper to be presented at the 65th Annual AWS Convention in Dallas, Texas, during April 8-13, 1984.

M. J. CIESLAK, formerly a Steel Founders' Society Graduate Fellow at Rensselaer Polytechnic Institute, is now a Member of the Technical Staff, Sandia National Laboratories, Albuquerque, New Mexico; A. M. RITTER is Staff Metallurgist, General Electric Corporate R&D, Schenectady, New York; and W. F. SAVAGE is Professor of Metallurgy and Director of Welding Research, Rensselaer Polytechnic Institute, Troy, New York.

**Melting wherein heat, stirring and support are provided by magnetic fields from coils surrounding the metal.*

Table 1—Compositions of Heat Materials Supplied by the Steel Founders' Society of America, Wt-%

	Heat number			
	1	2	3	4
C	0.08	0.04	0.06	0.10
Mn	0.60	0.21	1.17	0.30
Si	1.05	0.38	0.60	0.69
Ni	13.20	15.38	12.08	10.62
Cr	18.32	19.55	18.18	20.31
Mo	2.26	2.88	2.48	2.34
N	0.04	0.04	0.05	0.05
S	0.016	0.025	0.016	0.032
P	0.035	0.036	0.027	0.046

1697°F). Brandis *et al.* (Ref. 12) reported similar data for an entire range of Cr-Mo ferritic stainless steels. Chi phase did not appear in an Fe-20Cr-2Mo alloy until 500 h when heat-treated at 700°C (1292°F), the nose of the TTP diagram for that alloy.

In addition, Kautz and Gerlach (Ref. 13) have reported finding chi phase as an eutectic constituent in niobium-containing Type 316 stainless steel, which was heat treated at 1380°C (2516°F) and water quenched. Omsen and Eliasson (Ref. 14) found chi phase as an eutectic constituent in 50 kg (110 lb) castings of Type 316L stainless steel. They also reported that nitrogen additions did not influence the existence of eutectic chi phase in that alloy.

Based on the data available in the literature, it may be said that chi phase formation in the solid state generally is enhanced by increasing molybdenum content, increasing chromium content when molybdenum is held constant, and decreasing nitrogen content. Chi phase has been reported to form in the temperature range of 649-950°C (1200-1742°F). In addition, chi has been found as an eutectic constituent in alloys that had been processed with comparatively slow solidification rates.

Table 2—Alloy Ferrite Contents

Heat number	Material condition	Magne-Gage ferrite number
1	As-received	0.2
1	Welded using 100% Ar	0.2
1	Welded: 94% Ar-6% N_2	0
2	As-received	2.6
2	Welded using 100% Ar	2.3
3	As-received	3.0
3	Welded using 100% Ar	5.4
3	Welded using 99% Ar-1% N_2	1.3
3	Welded 97% Ar-3% N_2	0.5
3	Welded using 94% Ar-6% N_2	0.1
4	As-received	14.0
4	Welded using 100% Ar	17.3

Materials

The compositions of heats used for the study described in this paper are given in Table 1. The materials were supplied by the Steel Founders' Society of America in the form of solution-annealed keel block legs. Specimens were machined from these castings as described previously (Ref. 15).

Table 2 gives the ferrite contents of the alloys in both the as-received condition and after welding, using the indicated shielding gas mixtures.

Experimental Procedure

Cooling Rate Measurements

Cooling rate experiments were performed using the thermocouple plunge method developed by Dorschu (Ref. 16). In this method, open circuit type, bare wire, W3Re-W25Re thermocouples were thrust into the trailing edge of a moving GTA weld pool by a solenoid-triggered, spring-loaded mechanism, as shown schematically in Fig. 1. The thermocouple was then allowed to freeze in place, in order to record the cooling rates associated with solidification and subsequent cooling to room temperature.

A Honeywell direct recording oscillograph was used to record the voltage/time profiles. All necessary cold junction corrections were made to the data subsequent to recording. Figure 2 shows the position of the thermocouple/sheath in the weld after testing is complete.

It must be stated that cooling rates within a weld vary from position to position, and that this method samples temperature over the distance separating the two thermocouple wires. Nevertheless, based on previous investigations (Refs. 16,17,18), it was felt the data were representative for the particular welding parameters.

The welding variables used during cooling rate measurements are given in Table 3; they were the same as those used during earlier Varestraint testing of

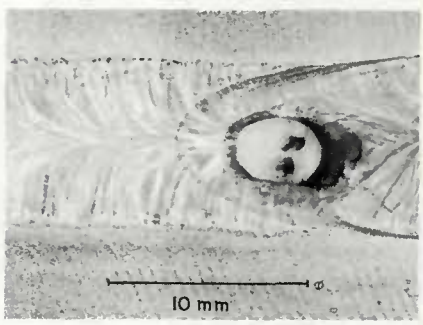

Fig. 2—Macrograph of thermocouple after insertion into weld pool. Heat 3, 97% Ar-3% N_2 shielding gas

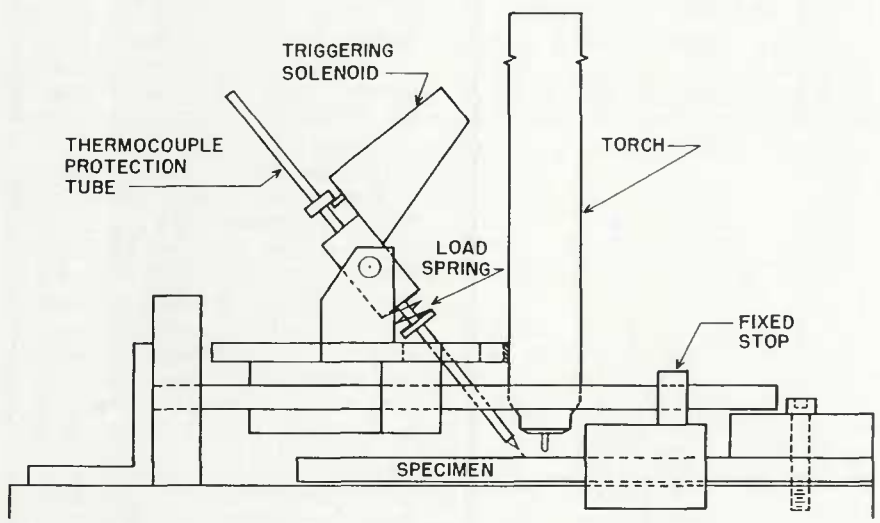

Fig. 1—Schematic side view of thermocouple plunging device

Table 3—Gas Tungsten Arc Welding Conditions Using DCSP

Current, A	250
Voltage, V	12.5
Torch travel speed, ipm (mm/s)	4 (1.69)
Electrode	W-2% ThO_2, ground to conical tip with a 90 deg apex angle
Gas flow rate, cfh (L/min)	40 (18.9)
Gas composition	See text
Electrode-to-work distance,[a] in. (mm)	3/32 (2.38)

(a) Measured cold.

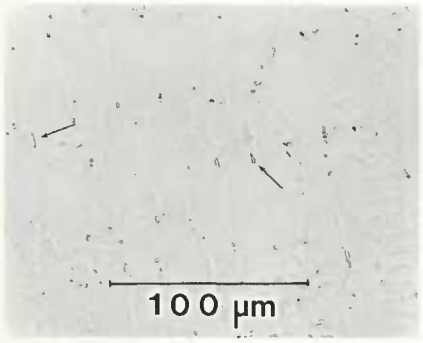

Fig. 3—Micrograph of weld metal, heat 1, 100% Ar shielding gas, primary austenite mode. Arrow denotes position of eutectic ferrite

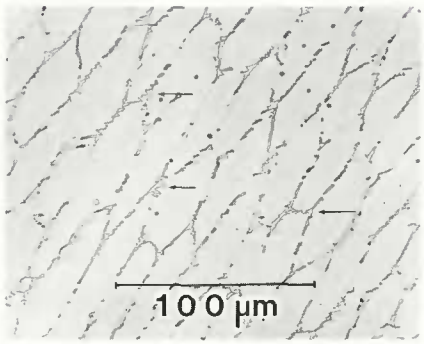

Fig. 4—Micrograph of weld metal, heat 2, 100% Ar shielding gas, primary austenite mode. Arrow denotes position of eutectic ferrite

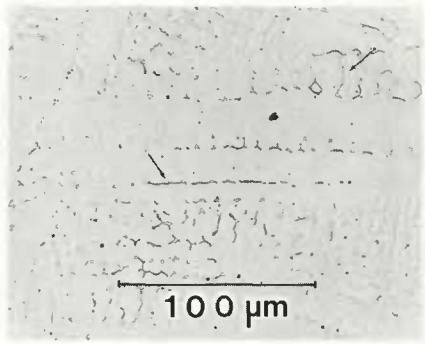

Fig. 5—Micrograph of weld metal, heat 3, 99% Ar–1% N_2 shielding gas, primary austenite mode. Arrow denotes position of eutectic ferrite

the same alloys (Ref. 19). Furthermore, the thermocouple was inserted into the trailing edge of the weld pool at the position where the pool would have been located at the instant of straining during a Varestraint test. This is the position from which extraction replicas were taken on Varestraint specimens for microanalysis.

Optical and Electron Microscopy

Specimens for optical microscopy were cut from Varestraint bars and included the hot cracks present. These specimens were subsequently mounted in epoxy, polished through 0.05 micron (1.9×10^{-6} in.) alumina, and etched using a 10% oxalic acid electroetch.

Thin foils for analytical electron microscopy (AEM) were prepared from the weld metal of Varestraint specimens. Extraction replicas were made in order to separate the chi phase from the surrounding matrix, using a two-stage acetylcellulose tape technique described elsewhere (Ref. 20). Etching of the surfaces prior to extraction replication required the use of one or two solutions, including an acid ferric chloride etch (5 gm $FeCl_3$/ 50 ml HCl/100 ml H_2O) and an aqua regia type etch (10 ml HNO_3/10ml acetic acid/ 15 ml HCl).

Extraction replicas and thin foils were examined in a JEOL JSEM-200 scanning transmission electron microscope (STEM) operated at 200 kV. The JSEM-200 is equipped with a Nuclear Semiconductor energy dispersive x-ray detector and a Tracor Northern NS880 analyzer for data acquisition and reduction. A Tracor Northern software package was used to subtract the background counts and integrate the remaining counts in each peak. The beam size used during spectra acquisition was approximately 100Å. The procedure for conversion of integrated intensities to weight-percentages has been described previously (Ref. 21). Constants used were assumed to be applicable over a wide range of compositions.

Results and Discussion

Austenitic stainless steels may solidify either as primary delta-ferrite or as primary austenite, depending to a large extent on the nominal chemical composition.

The primary austenite solidification mode occurs in alloys having a relatively high ratio of austenite stabilizing elements (Ni, C, N, Mn, *etc.*) to ferrite stabilizing elements (Cr, Mo, Si, Nb, *etc.*). Austenite is the first phase to crystallize from the liquid. Any ferrite present in the microstructure formed from the liquid during the final stages of solidification, in interdendritic and intergranular volumes, and is referred to as eutectic ferrite.

The primary delta-ferrite solidification mode occurs in those alloys having a relatively high ratio of ferrite stabilizers to austenite stabilizers. Delta-ferrite is the first phase to form from the liquid. Austenite may also crystallize from the liquid, but at a later stage of solidification. In addition, the primary delta-ferrite dendrites attempt to transform to the equilibrium austenite phase as the temperature falls. The incomplete nature of this transformation results in a microstructure consisting of the remnants of the original delta-ferrite dendrites in an austenite matrix. This residual delta ferrite often has a vermicular or lathy morphology. The details of the mechanics of solidification and subsequent solid-state transformation in this class of alloys has been discussed earlier (Refs. 19,21).

The solidification mode of a primary delta-ferrite duplex stainless steel may be changed to primary austenite by the addition of nitrogen to the argon shielding gas during GTA welding (Ref. 19). It has been shown that an increase in hot cracking susceptibility accompanies this shift in solidification mode. Furthermore, a change in the microstructure and in the pattern of microsegregation resulted; this allowed a difference to be found between the remnants of primary delta-ferrite dendrites and the residual eutectic ferrite.

Optical micrographs representative of the weldment microstructures studied are shown in Figs. 3–7. Figures 3, 4, and 5 are micrographs of welds which solidified as primary austenite. Arrows denote the position of interdendritic eutectic ferrite. Figures 6 and 7 show the microstructure associated with primary delta-ferrite solidification; the dark etching phase is the residual delta-ferrite.

Solid State Chi Phase

Figure 8A is a TEM micrograph of eutectic ferrite found in the weld metal of heat 2 welded using 100% Ar shielding gas. The precipitates appearing at the eutectic ferrite/austenite interface are shown at higher magnification in Fig. 8B.

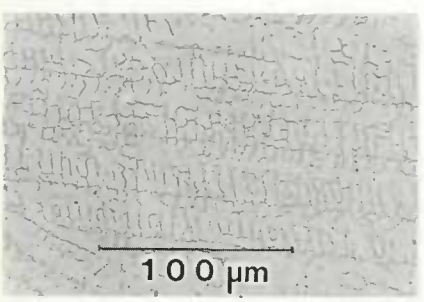

Fig. 6—Micrograph of weld metal, heat 3, 100% Ar shielding gas, primary delta-ferrite mode

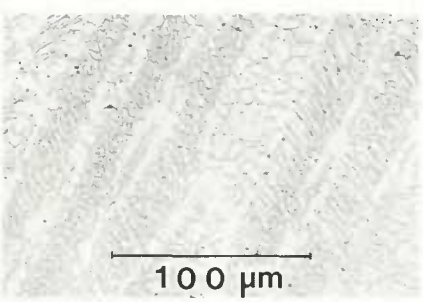

Fig. 7—Micrograph of weld metal, Heat 4, 100% Ar shielding gas, primary delta-ferrite mode

Fig. 8—Thin foil TEM micrographs of weld metal, heat 2, 100% Ar shielding gas. A—small chi precipitates at eutectic ferrite/austenite interface, primary austenite mode; B—same area as in "A" showing the extent of chi precipitation at the eutectic ferrite/austenite interface

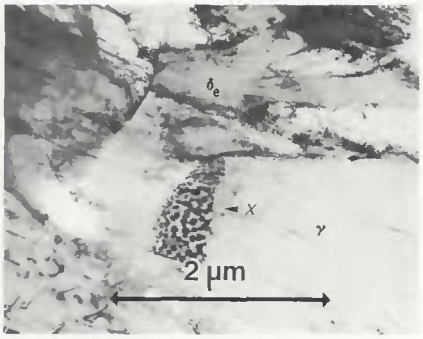

Fig. 9—TEM thin foil micrograph of weld metal, heat 3, 97% Ar-3% N_2 shielding gas, showing chi phase precipitates at eutectic-ferrite/austenite interface; primary austenite mode

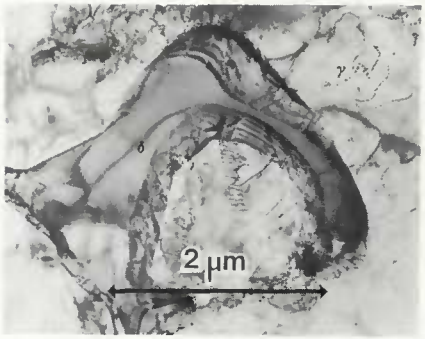

Fig. 10—TEM thin foil micrograph of weld metal, heat 3, 100% Ar shielding gas showing precipitate-free delta-ferrite/austenite interface; primary delta-ferrite mode

Selected area electron diffraction patterns from these precipitates were indexed to chi phase.

Similar chi phase precipitation was observed along the eutectic ferrite/austenite interfaces in heat 3 welds made using 97%Ar-3%N_2 shielding gas, as shown in Fig. 9. Chi phase was also observed at similar positions in heat 3 welds which were produced using 99% Ar-1%N_2 and 94%Ar-6%N_2 as the shielding gases.

All of the above mentioned welds solidified as primary austenite with the only ferrite present being of the eutectic type. Interestingly, no chi phase was found at the delta-ferrite/austenite interfaces in heat 3 welds when pure argon was used as the shielding gas. The solidification mode in this case was one of primary delta-ferrite. Figure 10 is a representative TEM micrograph of the residual delta ferrite in these welds, showing a precipitate-free delta-ferrite/austenite interface.

The difference in segregation patterns resulting from the primary delta ferrite and primary austenite solidification modes can be seen by comparing the STEM profiles shown in Figs. 11 and 12, respectively. The eutectic ferrite is enriched in molybdenum relative to the residual primary delta-ferrite and austenite, and enriched in nickel relative to the primary delta ferrite.

Diffusion data available for nickel and chromium in stainless steels (Refs. 22-26) indicate that, with the cooling rates present in GTA welding, the extent of structure and composition modifications in weldments of these materials is minimal at temperatures below 1100°C (2012°F). Recent work by Ritter (Ref. 27) on Nitronic 50 steel has shown that the composition and volume fraction of ferrite is not significantly altered below 1100°C (2012°F). Vitek and David (Ref. 28) have similarly shown by isothermal heat treatments of duplex alloys that the time necessary for alloy structure and composition modification at 1000°C (1832°F) is far greater than is possible during cooling associated with conventional arc welding processes.

The implication is that the form and composition of the ferrite at 1000°C (1832°F) is not significantly different than at room temperature in as-welded microstructures. Therefore, as the weld metal

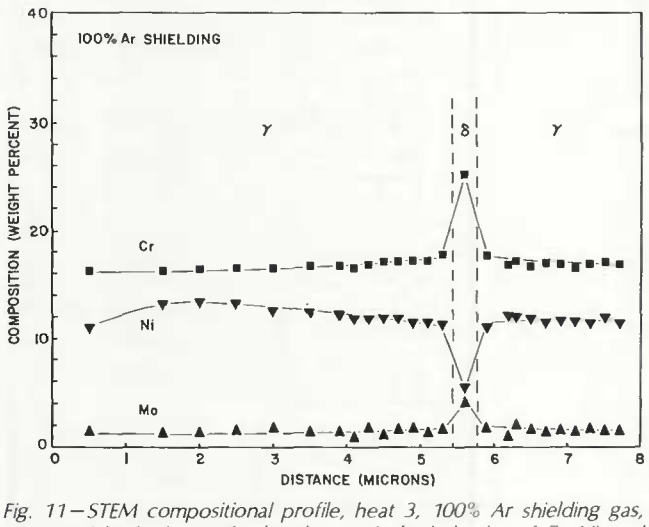

Fig. 11—STEM compositional profile, heat 3, 100% Ar shielding gas, primary delta-ferrite mode showing particular behavior of Cr, Ni, and Mo

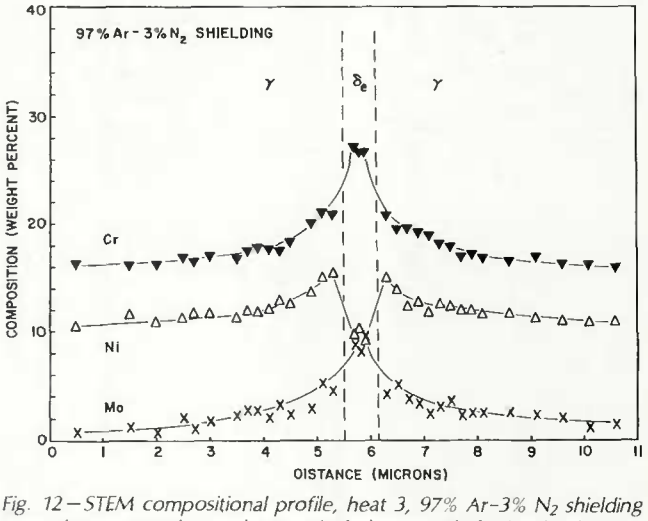

Fig. 12—STEM compositional profile, heat 3, 97% Ar-3% N_2 shielding gas, primary austenite mode. Area includes eutectic ferrite, δ_e, showing particular behavior of Cr, Ni, and Mo. Note difference in Ni profile, and Mo content of δ_e in comparison with Fig. 11

cools through the solid state chi formation range, the ferrite present has the composition shown in either Figs. 11 or 12. Lyman *et al.* (Ref. 29) and Brooks *et al.* (Ref. 30) have shown by high resolution STEM/EDS analyses that the Cr content in the residual room temperature primary delta ferrite is at a maximum adjacent to the ferrite/austenite interface. The enrichment was found to be of the order of 1 wt-%.

This phenomenon was explained by Cieslak *et al.* (Ref. 19) as being a direct consequence of the nonequilibrium nature of the incomplete diffusion-controlled ferrite-to-austenite transformation. Furthermore, it was postulated in the same study that molybdenum would show similar behavior, as it too is a ferrite stabilizer. The partitioning of molybdenum during transformation was found to be similar to but greater in relative amounts than that found for chromium.

Since eutectic ferrite is also a nonequilibrium phase at room temperature, partial transformation of this phase to austenite should occur during cooling of the weldment. The incomplete nature of this transformation is also the result of a lack of sufficient time at temperature. It can be postulated that the distribution of alloying elements in this ferrite would be similar to that found in the residual primary delta ferrite since both are subjected to the same type of transformation at approximately the same cooling rates. However, to date high resolution STEM/EDS profiles within the eutectic ferrite have not been performed to confirm this postulate.

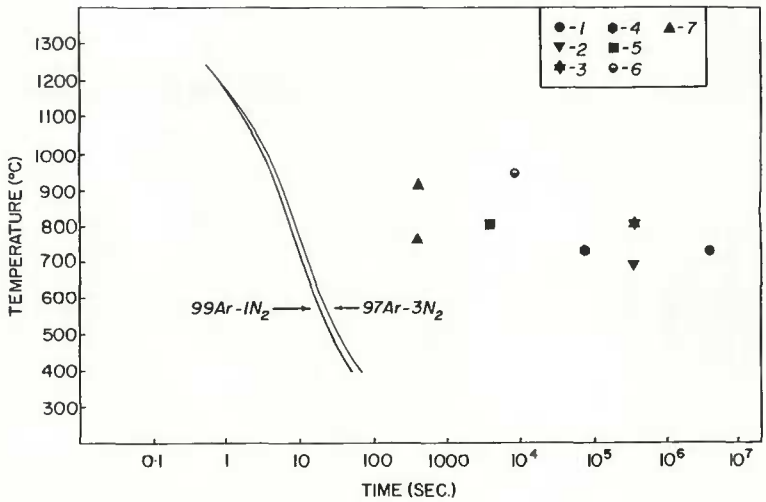

Fig. 13—Comparison of literature isothermal chi formation data (points) with representative measured cooling curves from weld metal of heat 3. Shielding gases as shown

The occurrence of chi phase in the solid state in alloys containing eutectic ferrite can now be explained. The kinetics of chi formation are greatly enhanced by the presence of molybdenum. Brandis *et al.* (Ref. 12) have shown that chi phase formation in Fe-24Cr-5Mo occurs at least 3 orders of magnitude faster than in Fe-24Cr-2Mo ferritic stainless steel. Thus, the high Mo content in the eutectic ferrite is the driving force for the precipitation of chi phase. The postulated Mo enrichment near the interface would make this region even more likely to be the starting point for chi phase precipitation.

Cooling rate measurements, as described earlier, were made in welds of these alloys in order to compare the weld thermal cycles with isothermal transformation data. Table 4 gives a compilation of various studies on the kinetics of chi phase precipitation in a group of relevant alloys. The time of earliest chi phase precipitation in the table represents the nose of the isothermal transformation diagram found in the study referenced, or simply the earliest chi phase appearance found if an entire diagram was not developed.

Cooling curves representative of the data generated in the present study are drawn in Fig. 13. The numbered symbols in Fig. 13 refer to the numerical order of data in Table 4. The Brandis data (point 7)

Table 4—Compilation of Studies on Chi Phase Precipitation Kinetics

Study no.	Material, condition	Composition	Earliest chi, h	Temperature, °C (°F)	Reference
1	16-8-2, cast duplex austenite-ferrite	Fe-16.4Cr-8.7Ni-1.64Mo-0.04C	1000	732 (1350)	Ref. 2—J.M. Leitnaker, *Weld. Jour.* 61(1):9-s to 12-s.
2	24-2 ferritic SS, annealed 30 min at 1000°C (1832°F)	Fe-23.5Cr-2.1Mo	100	700 (1292)	Ref. 12—H. Brandis *et al.*, *Arch. Eisen.*, 1975, 46(12): 799-804.
3	316 austenitic SS, annealed 1½ h at 1260°C (2300°F)	Fe-17.4Cr-12.3Ni-2.05Mo-0.07C	100	815 (1499)	Ref. 4—B. Weiss, R. Stickler, *Met. Trans.*, vol. 3, no. 4, April 1972, 851-866.
4	316Ti austenitic SS, annealed at 1204°C (2199°F), 10% reduction in area by swaging	Fe-17.5Cr-14.0Ni-2.51Mo-0.29Ti-0.06C	20	770 (1418)	Ref. 8—A. Grot, J. Sprueill, *Met. Trans.*, vol. 6A no. 11, Nov. 1975, 2023-2030.
5	316L austenitic SS, annealed 1½ h at 1260°C (2300°F)	Fe-17.3Cr-13.1Ni-2.66Mo-0.02C	2	950 (1742)	Ref. 4—B. Weiss, R. Stickler, *Met. Trans.*, vol. 3, no. 4, April 1972, 851-866.
6	28-4-2 ferritic SS, annealed 1 hr at 1093°C (1999°F)	Fe-28.5Cr-4.2Mo-2.0Ni-44ppmC-110ppmN	1	815 (1499)	Ref. 10—M. Streicher, *Corr.*, vol. 30, no. 4, April 1974, 115-124.
7	24-5 and 28-5 ferritic SS, annealed 30 min at 1000°C (1832°F)	Fe-24.0Cr-4.83Mo	Less than 6 min	750-925°C (1382-1697°F)	Ref. 12—H. Brandis *et al.*, *Arch. Eisen.*, 1975, 46(12), 799-804.
		Fe-28.0Cr-4.93Mo	Less than 6 min	750-925°C (1382-1697°F)	

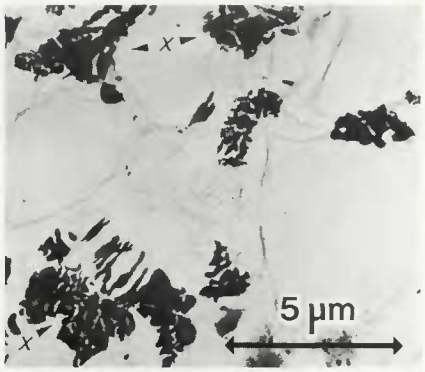

Fig. 14—Extraction replica TEM micrograph from a hot crack in heat 1, 100% Ar shielding gas, showing eutectic chi phase along the crack; primary austenite mode

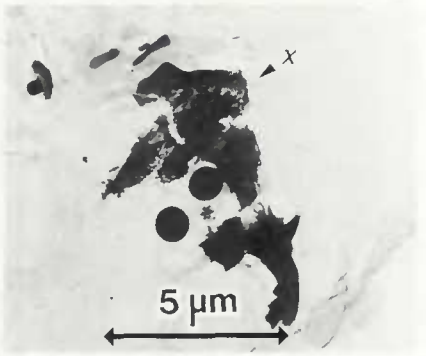

Fig. 15—Extraction replica TEM micrograph from a hot crack in heat 2, 100% Ar shielding gas, showing eutectic chi phase (arrow) along the crack; primary austenite mode

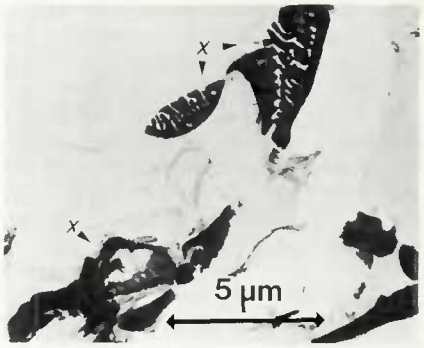

Fig. 16—Extraction replica TEM micrograph from a hot crack in heat 3, 97% Ar-3% N_2 shielding gas, showing eutectic chi phase (arrow) along the crack; primary austenite mode. Note the lamellar appearance of the chi phase

indicated that chi phase was already found after the minimum heat treatment time of 6 min. The corresponding isothermal transformation diagram indicated that the nose of the curve would probably occur at a much shorter time and at a temperature of about 900°C (1652°F).

The alloys tested in the present study passed through the chi formation temperature range in less than 10 seconds(s), and the eutectic ferrite had a Mo content at least equivalent to, and generally higher than, the alloys investigated by Brandis *et al.* (Ref. 12). It is, therefore, not surprising to find chi phase forming during cooling of this kind of duplex structure.

Chi phase was not found associated with the remnants of primary delta-ferrite. Figure 11 indicates that the Mo content of this ferrite is substantially lower than that of the eutectic ferrite shown in Fig. 12. This is related to the fact that the segregation accompanying the two modes of solidification is different. The composition of the two types of ferrite at the solidus temperature and the ferrite starting point compositions prior to the diffusion transformation of ferrite-to-austenite would, therefore, be different. The kinetics of chi formation are such that cooling rates found in the primary delta-ferrite welds are too fast to allow precipitation with the Mo contents present in this form of ferrite.

Nitrogen additions to austenitic stainless steels have been shown to retard the formation of chi phase in the solid state (Ref. 6). In the study described in this paper, chi phase was formed when the solidification mode of heat 3 was switched to primary austenite by the addition of nitrogen to the weld metal via the shielding gas.

The addition of nitrogen resulted in a major element segregation pattern, which enhanced the kinetics of chi phase formation. Furthermore, the vast majority of the nitrogen added would probably partition to the austenite present because of the much higher solubility of nitrogen in the face-centered-cubic austenite phase (Refs. 31,32). The previously reported (Ref. 6) nitrogen effect in fully austenitic stainless steel does not apply in this duplex case. Also, chi phase precipitation in heats 1 and 2, welded using 100% Ar, indicates that nitrogen additions are not necessary for the formation of this phase.

The morphology of the chi precipitates is evidence of a rapid cool through the chi formation temperature range. Many nucleation events occurred at the austenite/eutectic-ferrite interfaces, indicating that a relatively large degree of undercooling occurred before nucleation began. Subsequent growth and/or coalescence of the many chi particles was severely limited as a result of insufficient time at temperature.

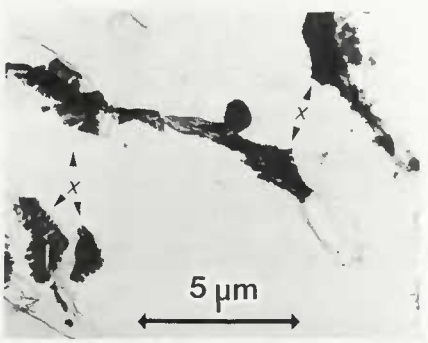

Fig. 17—Extraction replica TEM micrograph from a hot crack in heat 4, 100% Ar shielding gas, showing eutectic chi phase (arrow) along the crack; primary delta-ferrite mode

Eutectic Chi Phase

Extraction replicas prepared from hot cracked Varestraint specimens revealed a morphologically distinct form of chi along the sides of and within hot cracked solidification grain boundaries. Figures 14, 15, 16, and 17 are from extraction replicas of hot cracks in heats 1, 2, 3, and 4, respectively, welded using the shielding gases given in each caption.

Chi phase can be seen in Figs. 14-17. This branched, lamellar type of chi phase has been found by Kautz and Gerlach (Ref. 13) along liquated grain boundaries in stainless steel specimens heat-treated at 1380°C (2516°F). Omsen and Eliasson (Ref. 14) found eutectic chi phase in large stainless steel castings. However, these investigators observed chi phase after solidification which had occurred far more slowly than in the present study.

Honeycombe and Gooch (Ref. 33) observed a liquated phase in Type 316 stainless steel weld metal and found the phase to be somewhat higher in Si and Cr, and significantly higher in Mo, than the surrounding matrix. Although they did not identify this phase, they published SEM micrographs which showed the phase to be remarkably similar in morphology to the eutectic chi phase shown in Figs. 14-17.

Eutectic chi was observed in welds that solidified either as primary austenite or as primary delta-ferrite. The segregation of chi-forming elements along solidification grain boundaries was great enough to enable chi phase to form directly from the liquid.

Chi Phase Chemistries

Analytical electron microscopy techniques were used to determine the chemical compositions of the chi phase found in the various positions in the weld metal. The method of calculating the phase chemistry from AEM spectra has been described previously (Ref. 21).

Table 5 lists the various compositions determined from the experimental data. It must be pointed out that the data represent mean compositions only and that a substantial scatter in the data exists around these mean values. The determination of the nickel content, for example,

involved measuring relatively low numbers of counts; the relative error is, therefore, necessarily higher than in the case of iron and chromium.

The molybdenum content was determined using a constant acquired on a Type 316 stainless steel standard, which may contain an order of magnitude less molybdenum than the chi phase found here. Extrapolation of this constant may also lead to some systematic errors.

The EDS spectra also showed evidence of silicon present in the chi phase, to a small extent. This was not taken into account in the determination of phase composition, because it was felt that a constant for silicon could not be confidently determined from the standard used in this study. Some carbon could also have been dissolved in the chi phase, but this could not be detected by our method of analysis.

The errors inherent in this kind of analysis are most readily apparent by noticing in Table 5 that the weight percentages combine to less than 100% in all cases. Nevertheless, the relative amounts of the four major elements in the chi phase can be determined and compared with confidence.

Inspection of Table 5 reveals that, in general, the average molybdenum content of the solid state chi phase is greater than that found in the chi phase extracted from the hot cracks. We refer to chi in the hot cracks as such, instead of as eutectic chi, because occasionally chi was found in this region as small distinct particles similar to solid state chi. It is possible that these particles are in reality solid state chi, which was extracted from eutectic-ferrite present in the vicinity of the crack. If this is true, the actual compositions of the two forms of chi may differ to an even greater extent than shown in Table 5.

The compositions of the solid state chi phase tend towards the stoichiometry reported by Weiss and Stickler (Ref. 4) for chi formed during a solid state transformation. In addition, the eutectic chi found by Kautz and Gerlach (Ref. 13) had a stoichiometry quite similar to that found in this study for chi in the hot cracks. An effort is continuing to develop a larger statistical base for chi phase compositional data and to relate composition better to morphology, especially in the hot cracked areas.

Chi phase can form directly from the liquid in these alloys because the molybdenum content necessary to form eutectic chi is of the order of 10 wt-% less than is required to form solid state chi. Local molybdenum segregation along solidification grain boundaries is apparently ample in either solidification mode for alloys of this type, containing nominally 2–3 wt-% Mo.

Table 5—Chi Phase Chemistries

Heat no.	Shielding gas	Primary solidification mode	Mean Chi composition, wt-%
Solid State Chi:			
1	100% Ar	Austenite	32Cr-37Fe-19Mo-5Ni
2	100% Ar	Austenite	27Cr-35Fe-28Mo-4Ni
3	97% Ar–3% N_2	Austenite	26Cr-45Fe-20Mo-4Ni
Weiss & Stickler (Ref. 4)	–	–	21Cr-52Fe-22Mo-5Ni
Chi Along Hot Cracks:			
1	100% Ar	Austenite	32Cr-44Fe-12Mo-8Ni
1	94% Ar–6% N_2	Austenite	31Cr-47Fe-10Mo-9Ni
2	100% Ar	Austenite	29Cr-53Fe-6Mo-8Ni
3	97% Ar–3% N_2	Austenite	29Cr-47Fe-13Mo-6Ni
4	100% Ar	Delta-ferrite	34Cr-47Fe-10Mo-9Ni
Kautz & Gerlach (Ref. 13)	–	–	28Cr-55Fe-12Mo-5Ni[a]

[a]Assuming 3 atomic-percent nickel.

Closure

The occurrence of chi phase as an eutectic constituent is of interest, since small volume fractions of an eutectic constitutent can cause hot cracking problems if the constituent has a sufficiently low melting point and low surface tension. The effect of elements such as phosphorus, sulfur, and silicon on stainless steels which solidify as primary austenite is detrimental and well documented. In the study described in this paper, a measurement of the direct effect of eutectic chi on hot cracking sensitivity could not be determined because of the complicating effects of the residual elements named above. An experiment on ultra high purity Type 316 stainless steel is under way to isolate this effect.

Independent of the hot cracking problem, chi phase can be an embrittling phase. With respect to mechanical properties and fracture, either type of chi phase found in the microstructure is unwanted. Eutectic chi phase may be particularly insidious, as it forms along the grain boundaries in the solidifying weld metal. Weiss and Stickler (Ref. 4) found that the presence of chi did not reduce the impact properties of Type 316 stainless steel at liquid nitrogen temperatures; however, $M_{23}C_6$ carbides were present in that microstructure so that the effect of chi alone could not be measured. In addition, eutectic chi was not present in that study, and this form of chi has not been thoroughly investigated.

Conclusions

1. Chi phase has been found in as-solidified CF-8M weld metal.

2. Chi phase precipitates in the solid state as a result of the high Mo content of the eutectic ferrite. This type of chi phase forms on the austenite/eutectic-ferrite interfaces.

3. Chi phase was not found associated with residual primary delta-ferrite as a result of the lower Mo content of this ferrite.

4. A morphologically distinct and chemically distinguishable type of chi phase forms as an eutectic constituent at solidification grain boundaries in welds solidifying either as primary austenite or as primary delta-ferrite.

5. Eutectic chi phase was found along the sides of and within hot cracks, but the influence of this phase on hot cracking tendencies has not yet been isolated.

References

1. Kasper, J. S. 1954. *Acta Metallurgica* 2:456.

2. Leitnaker, J. M. 1982. Prevention of chi and sigma phases formation in aged 16-8-2 weld metal. *Welding Journal* 61 (1): 9-s to 12-s.

3. Lai, J. K., and Haigh, J. R. 1979. Delta-ferrite transformations in a Type 316 weld metal. *Welding Journal* 58 (1): 1-s to 6-s.

4. Weiss, B., and Stickler, R. 1972. *Metallurgical Transactions* 3 (4): 851.

5. Weigand, H., and Doruk, M. 1962. *Arch. Eisenhuttenw.* 8: 559.

6. Their, H., Baumel, A., and Schmidtmann, E. 1969. *Arch Eisenhuttenw.* 4: 333.

7. Spruiell, J. E., Scott, J. A., Ary, C. S., and Hardin, R. L. 1973. *Metallurgical Transactions* 4 (6): 1533.

8. Grot, A. S., and Spruiell, J. E. 1975. *Metallurgical Transactions* 6A (11): 2023.

9. Hull, F. C. 1973. Effects of composition on embrittlement of austenitic stainless steels. *Welding Journal* 52 (3): 104-s to 113-s.

10. Streicher, M. 1974. *Corrosion* 30 (4): 115.

11. Kiesheyer, H., and Brandis, H. 1981. *Corrosion resistance of high alloyed ferritic stainless steels.* Paper no. 126 presented at Corrosion/81, Toronto, Canada, April 6, 1981.

12. Brandis, H., Kiesheyer, H., and Lennartz,

G. 1975. *Arch. Eisenhuttenw.* 12: 799.

13. Kautz, H. R., and Gerlach, H. 1968. *Arch. Eisenhuttenw.* 2: 151.

14. Omsen, A., and Eliasson, L. 1971 (October). *Journal of the Iron and Steel Institute*: 830.

15. Cieslak, M. J., and Savage, W. F. 1980. Weldability and solidification phenomena of cast stainless steel. *Welding Journal* 59 (5): 136-s to 146-s.

16. Dorschu, K. E. 1968. Control of cooling rates in steel weld metal. *Welding Journal* 47 (2): 49-s to 62-s.

17. Arata, Y., Matsuda, F., and Katayama, S. 1977 (June). *Transactions of JWRI* 6 (1): 105.

18. Wen, J., Lundin, C. D., and Kruse, B. J. 1982. *Trends in welding research in the United States*, ed. S. A. David, p. 259. Metals Park, Ohio: American Society for Metals.

19. Cieslak, M. J., Ritter, A. M., and Savage, W. F. 1982. Solidification cracking and analytical electron microscopy of austenitic stainless steel weld metals. *Welding Journal* 61 (1): 1-s to 8-s.

20. Ritter, A. M., and Henry, M. F. 1982 (January). *Journal of Materials Science* 17: 73.

21. Ritter, A. M., Cieslak, M. J., and Savage, W. F. 1983 (January). *Metallurgical Transactions-A* 14A: 37.

22. Alberry, P. J., and Haworth, C. W. 1974. *Metal Science* 8: 407.

23. Hancock, G. F., and Leak, G. M. 1967. *Metal Science* 1: 33.

24. Perkins, R. A., Padgett, R. A., and Tunali, N. K. 1973. *Metallurgical Transactions* 4 (11): 2535.

25. Perkins, R. A. 1973. *Metallurgical Transactions* 4 (7): 1665.

26. Smith, A. F., and Hales, R. 1976. *Metal Science* 10: 418.

27. Ritter, A. M. 1982 (May). *Equilibrium phases in Nitronic 50 and Nitronic 50W stainless steels*. M.S. thesis. Troy, New York: Rensselaer Polytechnic Institute.

28. Vitek, J. M., and David, S. A. 1981. Microstructural analysis of austenitic stainless steel laser weld. Paper presented at 62nd Annual AWS Convention, Cleveland, Ohio, during April 5-10, 1981.

29. Lyman, C. E., Manning, P. E., Duquette, D. J., and Hall, E. 1978. *Scanning electron microscopy*, vol. I., p. 213.

30. Brooks, J. A., Williams, J. C., and Thompson, A. W. 1982. *Trends in welding research in the United States*, ed. S. A. David., p. 331. Metals Park, Ohio: American Society for Metals.

31. McGannon, H. E., ed. 1971. *The making, shaping, and treating of steel*, 9th ed., p. 330. United States Steel Corporation.

32. American Society for Metals. *Metals Handbook*, vol. 8, 9th ed., p. 422.

33. Honeycombe, J., and Gooch, T. G. 1970. *Metal Construction and British Weld. J.* 2 (9): 375.

American Welding Society 550 N.W. LeJeune Road, Miami, FL 33126 Telex: AMWELD SOC No: 51-9245
(305)443-9353

AN INVITATION TO AUTHORS

to present Brazing Papers at the
16th AWS International Brazing and Soldering Conference
Las Vegas, Nevada, April 30-May 2, 1985

The American Welding Society's C3 Committee on Brazing and Soldering invites you to present your outstanding and unpublished work in the field of brazing development, research or application at the 16th International AWS Brazing and Soldering Conference. This event will be held in conjunction with the Society's 66th Annual Convention at the Las Vegas Convention Center, Las Vegas, Nevada.

Please submit your abstract(s) by August 15, 1984, to be screened by the C3 Papers Selection Committee for the 1985 conference. Authors will be notified sometime in November, 1984, regarding acceptance of their papers.

Each abstract should be sufficiently descriptive to give a clear idea of the content of the proposed paper. In any case, it must contain not less than 500—*but preferably not more than 1000*—words. Manuscripts of approximately 5,000 words must be submitted before final approval is given. Repeated references to a company and/or the use of advertisement, trade names, trade marks (or expressions considered as such by the industry) are not permitted. Suitable generic terms must be used, in accordance with those standardized by the American Welding Society, where applicable.

Papers may be considered for publication in the *Welding Journal* regardless of acceptance for presentation at the conference. Topics of particular interest in brazing are:

Applied technologies of (1) aerospace structures, (2) machine tools, (3) nuclear assemblies, (4) automotive assemblies, (5) electronic equipment, (6) food processing equipment and (7) pressure vessels. Of special interest is the application of brazing to titanium, aluminum and other base metals including brazement strength data.

New research and development on (1) brazing filler metals, (2) brazing filler metal/base metal interaction, (3) nuclear properties of brazements, (4) electronic properties of brazements, (5) corrosion of brazements and (6) strength of brazed joints.

In addition, papers dealing with educational and informative aspects of brazing production, engineering, research and metallurgy are welcomed if the subject falls within the scope of the session.

Please fill out the Author's Application Form (reverse side), attach abstract thereto and return to AWS. To assure your paper's consideration for the 1985 conference, your abstract must be postmarked *no later than August 15, 1984.*

Paul W. Ramsey

Paul W. Ramsey
Executive Director

IMPORTANT: ABSTRACTS MUST BE AT LEAST 500 WORDS AND BE POSTMARKED NO LATER THAN AUGUST 15, 1984, TO ASSURE CONSIDERATION.

AUTHOR APPLICATION FORM
FOR
BRAZING PAPERS

DEADLINE AUGUST 15, 1984

Complete in Full and Return to American Welding Society, Inc., 550 N.W. LeJeune Road, Miami, Florida 33126

Date Mailed .....

Author's Name .....

Check how addressed: Mr. ☐

Title or Position ..... Ms. ☐ Dr. ☐ Other .....

Company or Operation .....

Mailing Address .....

City ..... State ..... Zip .....

Telephone (including Area Code) .....

If there are to be joint

Authorships, give name(s)

of other author(s)

Name .....

Address .....

Name .....

Address .....

Proposed title (10 words or less):

ABSTRACT:

- Type, double spaced, an abstract of *not less* than 500—but preferably not more than 1000—words on separate sheets and attach to this form.
- Be sure to give sufficient information to enable the Papers Selection Committee to obtain a clear idea of content of the proposed paper; confine background to about 100 words. Also be sure to *emphasize Results and Conclusions* since this material, together with information on what is NEW, will have a very important bearing on the final decision of the AWS C3 Papers Selection Committee.
- If complete manuscript is available, in addition to abstract, please attach two copies to this form.
- Application Form and Abstract must be postmarked not later than August 15, 1984, to assure consideration.

MANUSCRIPT DEADLINES:

- All manuscripts *must* be in the hands of the Papers Selection Committee no later than March 15, 1985. If received by that date, every effort will be made to publish them in a special Brazing and Soldering issue.
- It is expected that the Committee's selections will be announced sometime in November, 1984.
- If your paper is made a part of the program, which of the following manuscript deadlines will you be able to meet?
  December 15, 1984 ☐ January 14, 1985 ☐ February 15, 1985 ☐

PRESENTATION AND PUBLICATION OF PAPERS:

- Has material in this paper been previously presented in meeting or published?
  Yes ☐ No ☐ When? _____ Where? _____
- Following presentation at the *Conference,* would you accept invitations to present this paper before AWS Sections? Yes ☐ No ☐
- Papers accepted for presentation become the property of the Society with original publication rights assigned to the *Welding Journal.*

*RETURN TO AWS HEADQUARTERS. MUST BE POST-MARKED **NOT LATER THAN AUGUST 15, 1984,** TO ENSURE CONSIDERATION.*

Author's Signature